Article

Efficient Biosorption of Hexavalent Chromium from Water with Human Hair

Vivek Prakash, Kalpana Kumari, and Vibin Ramakrishnan*

Cite This: *ACS Omega* 2023, 8, 915−924

Read Online

ACCESS | Metrics & More | Article Recommendations | SI Supporting Information

ABSTRACT: The triphenyl group (trityl radical) possessing three-phenyl rings, self-assembled through aromatic $\pi-\pi$ stacking interactions, can form interesting crystalline organic nano-flowers. In this work, we have synthesized a hybrid material of 1,2-bis(tritylthio)ethane and magnetite, which reduces toxic Cr(VI) to non-toxic Cr(III). We validated the efficacy of the hybrid in reducing toxic Cr(VI) along with three other adsorbent systems. Among the five adsorbent systems tested, we observed that human hair has higher Cr removal efficiency, which prompted us to explore further using different mechanical forms of human hair. Pulverized hair (PH), hair powder (HP), and raw hair (RH) were evaluated by employing different reaction factors such as the adsorbent dose, pH, initial Cr(VI) concentration, and contact time. The comparative evaluation showed that PH has greater adsorption capacity (15.14 mg/g), followed by RH (13.27 mg/g) and HP (10.5 mg/g). While investigating the adsorption mechanism, we observed that it follows pseudo-second-order kinetics suggesting chemisorption. The Freundlich isotherm model fitted well for Cr(VI) adsorption by human hair, suggesting a multi-layered adsorption process. Overall, this study promises a cost-effective and eco-friendly bio-adsorbent for Cr(VI), which may be scaled up to design automated industrial waste disposal systems.
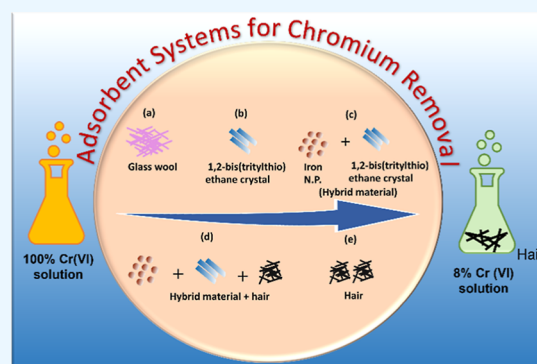
INTRODUCTION

Over the last few decades, waste water containing a significant amount of hexavalent chromium [Cr(VI)] has been expelled as industrial effluent, causing severe threat to the environment because of its mutagenic and carcinogenic side effects.[1] In aquatic systems, Cr(VI) present in solution as $HCrO_4$, CrO_4^{2-}, and $Cr_2O_7^{2-}$ is toxic to the environment.[2] In contrast, Cr(III) as Cr^{3+}, $Cr(OH)^{2+}$, $Cr(OH)_3$, and $Cr(OH)_4^-$ is less toxic and immobile.[3] Persistent exposure to Cr(VI) may even cause certain types of cancers in the gastrointestinal tract and lungs.[4] Therefore, removal of toxic Cr(VI) from the contaminated water is a crucial problem that has to be addressed effectively.

The permissible limit of the Cr(VI) contaminant in drinking water is 0.05 mg/L as per the World Health Organization (WHO). The Minimal National Standards (MINAS) upper limit for Cr(VI) in industrial waste is 0.1 mg/L. The industrial effluent waste may contain the Cr(VI) concentration which is much higher than the permissible range. Therefore, it is crucial to treat the water to attain its permissible Cr(VI) level. Several methods such as chemical precipitation,[5] photocatalysis,[6,7] coagulation,[8] oxidation,[9] and adsorption,[10] are in practice for heavy metal removal, and among them, adsorption is the most frequently used treatment technique. In photocatalysis, organic pollutants are degraded into small molecules, water, and carbon dioxide, whereas inorganic pollutants are either oxidized or reduced into nontoxic small molecules.[11] In the coagulation process, small particles are combined to form a

floc, and pollutants are adsorbed on its surface, which is removed by a solid separation method.[12] Over the years, the microwave-assisted catalyst for wastewater treatment has also been studied owing to its fast speed and non-thermal effect. Various low-cost adsorbents evolved from agronomic wastes,[13,14] natural materials,[15,16] and modified biopolymers[17−20] have been tested to remove heavy metals. However, none of them were very effective toward Cr removal. Therefore, a cheap, effective, and easily available adsorbent is essential for Cr removal.

Aromatic $\pi-\pi$ interaction or π stacking involves interaction of aromatic molecules, resulting in the formation of self-assembled molecules[21−24] which can be fabricated for various applications such as catalysts,[25] aggregation disruptors,[26] nanodots,[27] and artificial enzymes.[28] Our laboratory has earlier reported a novel organic molecule 1,2-bis(tritylthio)ethane which forms a rare organic nano-flower showing magnetic properties.[29,30] The nano-assembly was coated with magnetite nanoparticles to synthesize a functional trityl-magnetite hybrid
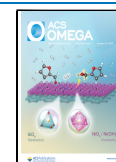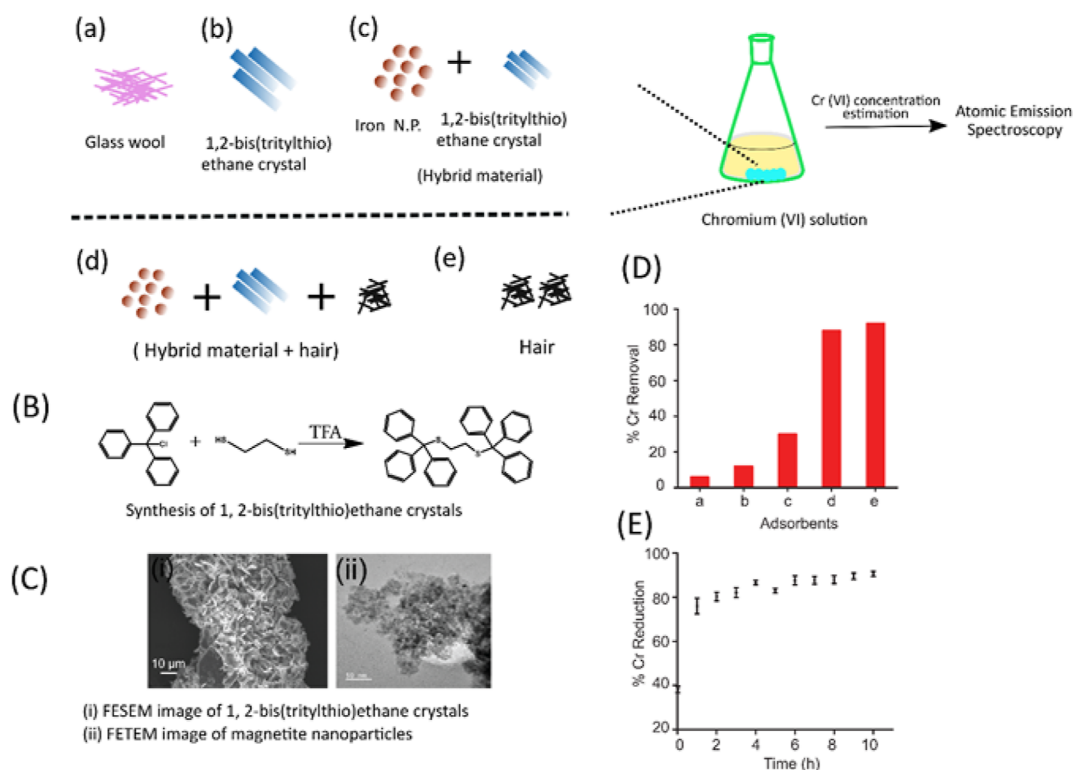
Figure 1. (A) Representative images of different adsorbent systems, (a) glass wool, (b) 1,2-bis(tritylthio)ethane crystal, (c) trityl-magnetite hybrid system, (d) hybrid material with human hair, and (e) human hair. (B) Synthesis of 1,2-bis(tritylthio)ethane crystals. Trityl chloride salt was incubated with EDT in the presence of TFA for 24 h. After 24 h, the obtained crystals were washed with diethyl ether. (C) (i) FESEM image of 1,2-bis(tritylthio)ethane crystals and (ii) FETEM image of magnetite nanoparticles. (D) Pilot experiment to verify different Cr adsorbent systems. (E) Reduction of Cr(VI) by the trityl-magnetite hybrid material. The hybrid material reduced up to 90% toxic Cr(VI) to nontoxic Cr(III).

material, which has resulted into a potent nano-adsorbent for the removal of toxic and heavy metal. In this study, we have evaluated the capacity of a trityl-magnetite hybrid material for Cr removal. As an extension of this investigation, we have evaluated the possibility of using different forms of human hair as the Cr removing bio-adsorbent. In a recently published report, human hair has been used as an adsorbent of oil from wastewater.[31,32] Basu and Mondal have investigated the utility of human hair as a Cr removal adsorbent by performing batch experiments.[32] In this study, we have further explored the possibility of employing different physical forms of human hair and compared their efficiency to remove Cr(VI).

RESULTS AND DISCUSSION

The steps involved in the synthesis of 1,2-bis(tritylthio)ethane crystals are shown in Figure 1B. The tri-phenyl methyl (trityl) group is a stable radical that was first described by Gomberg in 1900.[33] The positive charge on the α-carbon atom is "resonance-stabilized" by three aromatic rings. In the presence of an acid [trifluoroacetic acid (TFA)], trityl chloride generates free radicals which interact with 1,2-ethane dithiol (EDT) to form 1,2-bis(tritylthio)ethane. The field emission scanning electron microscopy (FESEM) image of the 1,2-bis(tritylthio)-ethane crystal and FE transmission electron microscopy (FETEM) image of magnetite nanoparticles are shown in Figure 1C. As shown in Figure 1C, magnetite nanoparticles formed a nanosphere-like structure. The FESEM image of 1,2-bis(tritylthio)ethane crystals in different pH ranges showed no significant difference in the morphology of the crystal

structure. This confirms the stability of 1,2-bis(tritylthio)-ethane under different pH conditions, which enables them to be used as an adsorbent under extreme pH conditions (Figure S1). In a set of preliminary experiments, we screened the Cr(VI) removal with various adsorbents such as glass wool, the 1,2-bis(tritylthio)ethane crystal, hair, and two hybrid materials (Figure 1A). Our results showed that the human hair has maximum adsorption as observed in experiments, followed by the hybrid material packed with hair. Compared to that of human hair, adsorption of other adsorbent systems was not appreciable. We observed relatively low Cr(VI) removal by 1,2-bis(tritylthio)ethane crystals and other adsorbents (Figure 1D). This prompted us to perform a series of experiments to verify the utility of human hair as a Cr(VI) adsorbent so as to develop it as an adsorbent system on a commercial scale.

Determination of Cr(VI) Reduction by the Trityl-Magnetite Hybrid Material. We evaluated the Cr(VI) reduction efficiency of magnetite-coated 1,2-bis(tritylthio)-ethane crystals (trityl-magnetite hybrid materials), which reduced Cr(VI) to Cr(III) with 90% efficiency (Figure 1E). It is reported that Fe(II) in magnetite nanoparticles reduces toxic Cr(VI) to the non-toxic form of Cr(III).[34] As the reaction progresses, the Cr(III) hydroxide or Cr(III)−Fe(III) complex is formed (i).[35] Sorption of Cr(VI) follows a two-step process: (i) electrostatic attraction of the Cr(VI) ion and then (ii) electron transfer between Cr(VI) and Fe(II).[36,37]
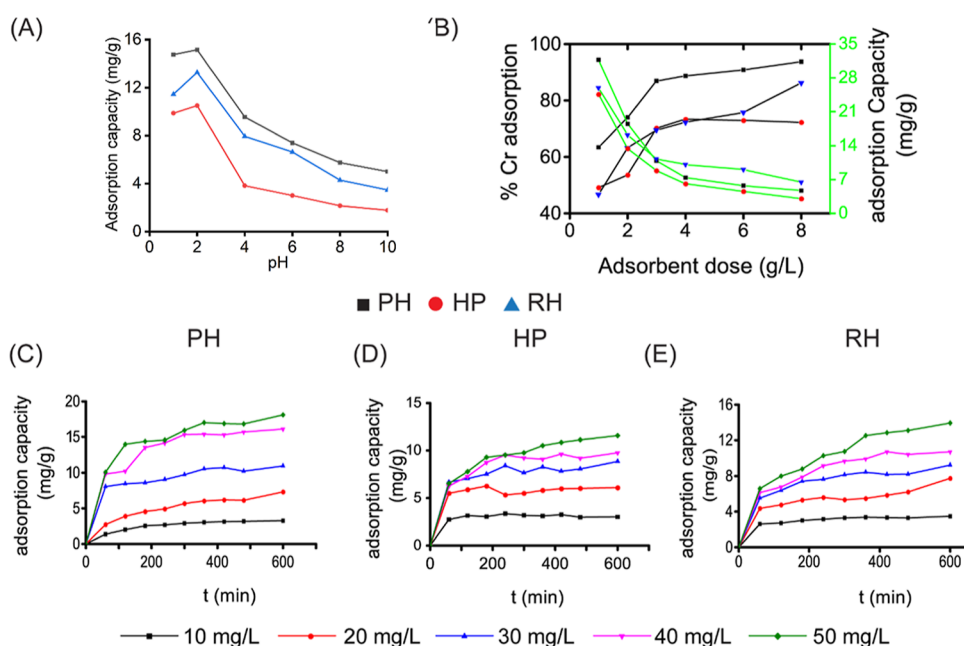
Figure 2. Efficiency of chromium adsorption: (A) effect of pH in modulating the adsorption capacity and (B) effect of adsorbent dose in modulating the adsorption capacity. Adsorption capacity (q_e) is calculated from the initial and final concentrations, volume of the solution, and weight of the adsorbent. Percentage adsorption (black) increases with increase in adsorption dose, while adsorption capacity (blue) decreases. Change in adsorption capacity with time for (C) PH, (D) HP, and (E) RH. Adsorption capacity increases with time and reaches saturation within 3 h, in almost all test cases. PH has approximately 80% adsorption capacity compared to RH and 50% compared to HP.

$$CrO_4^{2-} + 3Fe^{2+} + 3H_2O + H^+$$
$$\rightarrow CrOH^{2+} + 3Fe(OH)_2^+ \qquad (i)$$
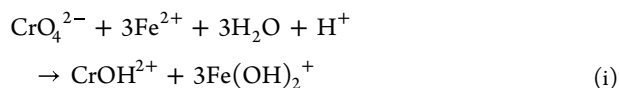
Characterization of Human Hair. Morphological characterization of adsorbents before and after Cr adsorption was performed by FESEM showing no significant structural change at the surface (Figure S2). The adsorption of Cr(VI) on hair is evident from the FESEM−energy-dispersive X-ray spectroscopy (EDX) analysis, suggesting that adsorption of Cr occurs on the surface of hair. Fourier-transform infrared (FT-IR) study was performed to determine the functional groups involved in the binding of Cr(VI) and analyzed by monitoring the deviation in the vibrational frequency (Figure S3).[38] Main components of human hair are proteins, water, and lipids. The IR spectrum of unprocessed hair has characteristic peaks resulting from the vibration of amide bonds in the peptide linkage of proteins in the range 1710−1595, 1585−1500, and 1310−1220 cm^{-1}. The prominent peak at 1637 cm^{-1} in all adsorbents is due to the amide I bond involving C=O stretching. We have observed no deviation of the 1637 cm^{-1} absorption peak in any adsorbent. The absorption peak in the range of 1510−1520 cm^{-1} is typical of amide II absorption. The absorption peak at 1449 cm^{-1} corresponds to the C−H stretching. The absorption peak at 1234 cm^{-1} corresponds to the amide III band which corresponds to the C−H stretching and N−H bending modes of vibrations. Absorption peaks due to the weak dioxide band (S=O$_2$) at 1114 cm^{-1}, the monoxide band at 1071 cm^{-1} (S−S=O), and the cysteic acid band at 1171 cm^{-1} were also observed.[39]

The efficiency of removal of Cr(VI) by using human hair at different pH was observed at an initial Cr(VI) concentration of 50 mg/L. Increase in Cr(VI) adsorption was observed with time and reached equilibrium in 3 h. The adsorption capacity of different adsorbents was observed to be different under different pH conditions. At pH 2, the calculated adsorption capacity of pulverized hair (PH) was 15.14, 13.27 mg/g for raw hair (RH), and 10.5 mg/g for hair powder (HP) (Figure 2A).

With increase in pH, the adsorption capacity was observed to be decreased. Higher absorption at low pH is due to the change in polarity of the adsorbents' surface as a result of change in pH of Cr(VI) solution. Cr(VI) exists in various forms such as H_2CrO_4, $HCrO_4^-$, CrO_4^{2-}, and $Cr_2O_7^{2-}$ in aqueous solution, and their stability differs with change in the pH. The active form of Cr(VI) adsorbed is $HCrO_4^-$, which is stable at only low pH, but the concentration of $HCrO_4^-$ decreases with increase in pH. Adsorbents get protonated at lower pH. Electrostatic attraction between $HCrO_4^-$ and the protonated adsorbent surface promotes adsorption of Cr-(VI).[40]

The study of the effect of the adsorbent dose on the adsorption of Cr at 25 °C is shown in Figure 2B. Results suggest that percentage removal of chromium increases with the increased adsorbent dose, whereas adsorption capacity decreases. On increasing the adsorbent dose from 0.5 to 8 g/L, the percentage Cr removal increased from 63% to approximately 94% for PH, 49 to 72% for HP, and 47 to 86% for RH. This occurs due to the accessibility of active binding sites with increased adsorbent dose.[41] Earlier reported observations suggest that decrease in adsorbent capacity is possible due to the aggregation of adsorbent particles and unbound sites present in adsorbents. As a result, the active sites are unable to be bound by metal ions.[42] The effect of the initial Cr concentration versus time is shown in Figure 2C−E for PH, HP, and RH, respectively. Cr adsorption efficiency of PH was found to be higher than that of HP and RH. This may be due to the more surface area of PH, compared to that of RH. The lower Cr(VI) adsorption by HP may be attributed to the loss of active sites during pyrolysis in the muffle furnace. It was found that there was very less increment in the Cr(VI)

adsorption after 3 h. Therefore, in all subsequent experiments, 3 h was regarded as the optimum contact time for the adsorption of Cr.

Adsorption Isotherm and Adsorption Kinetics. Adsorption isotherm and adsorption kinetics studies can provide significant insights while modeling specific treatment processes. The equilibrium constant and adsorption isotherm were measured at a constant adsorbent dose (100 mg), with varying initial Cr(VI) concentrations from 10 to 50 mg/L. The adsorption equilibrium was achieved by shaking Cr solution with adsorbents at 200 rpm. The relationship between q_e and C_e is shown in Figure S3. The Langmuir, Freundlich, and Dubinin−Radushkevich (D−R) isotherm models were adopted to characterize the adsorption capacity of the adsorbents (Figure 3). Parameters of the isotherm models are summarized
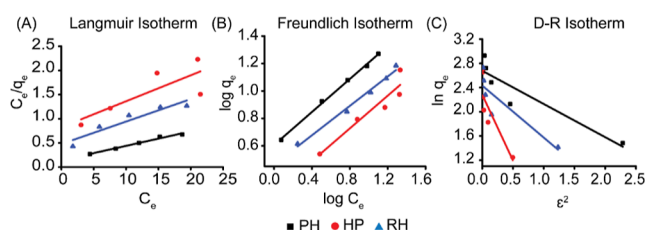
Figure 3. Adsorption isotherm for chromium adsorption. (A) Langmuir isotherm and (B) Freundlich isotherm and (C) Dubinin−Radushkevich (D−R) isotherm models for the possible mechanism of adsorption at equilibrium. Adsorption data fits well with the Freundlich isotherm model (R^2 = 0.99) compared to the Langmuir isotherm (R^2 = 0.94) and D−R isotherm (R^2 = 0.80). In the graph, C_e and q_e represent the equilibrium concentrations (mg/L) and adsorption capacity (mg/g) of different hair forms at 25 °C, respectively, whereas ε represents Polanyi potential.

in Table 1. The data suggests that the adsorption follows the Freundlich isotherm model (R^2 = 0.99). The value of adsorption intensity (n = 1.80) lying in the range of 1−10 confirms the favorable conditions for adsorption.[43] The mean biosorption energy (E) was evaluated using the D−R isotherm which gives crucial information on predicting the type of biosorption process. If E is less than 8 kJ/mol, the biosorption process is controlled by physisorption, whereas if E > 16 kJ/mol, chemisorption is followed. When value of E lies between 8 and 16 kJ/mol, the ion exchange process is followed.[44] In this study, the value of E for PH, HP, and RH was calculated to be 0.955, 0.479, and 0.763, respectively. The mean free energy obtained for this study is significantly less than 8 kJ/mol in all

the three cases. Although this data supports physisorption, the correlation with the D−R isotherm is relatively poor.

From Table 1, it may be observed that adsorption data fits well with the Freundlich isotherm model (R^2 = 0.99), compared to the Langmuir isotherm (R^2 = 0.94) and D−R isotherm (R^2 = 0.80). Therefore, the Freundlich model can describe the adsorption equilibrium more precisely.

Kinetics of metal interaction with the adsorbent surface was studied by pseudo-first-order kinetics, pseudo-second-order kinetics, and intra-particle diffusion. The relationship between q_t and t is shown in Figure S4. The adsorption data of all the three adsorbents PH, HP, and RH did not fit well with the pseudo-first-order kinetic model; instead, it clearly follows pseudo-second-order kinetics (R^2 > 0.98) (Figure 4, Table 2). Results, therefore, indicate that the adsorption occurs through chemisorption. The kinetic data were also analyzed using an intraparticle diffusion model indicating that the Cr(VI) adsorption occurs in two phases: the surface adsorption and intraparticle diffusion.[51] However, the kinetic data was not supportive of this assumption.

Desorption and Regeneration of Hair Samples. Repeated batch experiments have been performed to evaluate the reusability of the adsorbents. The reusability of adsorbents was tested by performing adsorption−desorption cycles of Cr(VI) up to three times using the same chromium solutions. The percentage Cr removal after regeneration was reduced to 40.12% for PH, 25.34% for HP, and 36.67% for RH (Table 3). The significant decrease in the removal percentage may be due to the non-availability of binding sites for chromium ions. The data, however, reaffirms the importance of pulverization while preparing hair as a possible adsorbent in commercially useable chromium purification systems.

Continuous Column Experiment. The batch adsorption study of Cr(VI) removal by different forms of hair suggested that the PH and RH adsorb Cr(VI) at appreciable levels. Further application of RH for Cr(VI) removal was evaluated through continuous column operations. The two predominant parameters which affect the breakthrough curve are the column height and flow rate. Here, we have tested the effect of different column heights at a flow rate of 5 mL/min and obtained a breakthrough curve as illustrated in Figure 5. The setup of the continuous column experiment is shown in Figure S5.

The different values from column experiments are shown in Table 4. The results showed that on increasing column height from 5 to 15 cm, the Cr removal capacity of the column increased from 47.67 to 57.80 mg/g. The breakthrough time

Table 1. Estimated Values of Parameters for Different Isotherm Models

isotherm model	parameters	PH	HP	RH
Langmuir	Q_0(adsorption capacity, mg/g)	27.94	18.60	21.52
	b(Langmuir constant, L/mg)	0.138	0.065	0.097
	R_L (separation factor)	0.42	0.60	0.51
	R^2 (coefficient of determination)	0.94	0.80	0.86
Freundlich	K_F (adsorption coefficient, L/g)	1.83	1.28	1.58
	$1/n_F$ (adsorption intensity)	0.60	0.59	0.53
	R^2 (coefficient of determination)	0.99	0.86	0.98
D−R	Q (adsorption capacity, mg/g)	14.53	9.78	11.37
	E (mean adsorption energy, kJ/mol)	0.955	0.479	0.763
	K (adsorption energy, mol²/J²)	5.49×10^{-7}	2.18×10^{-6}	8.58×10^{-7}
	R^2 (coefficient of determination)	0.80	0.67	0.69
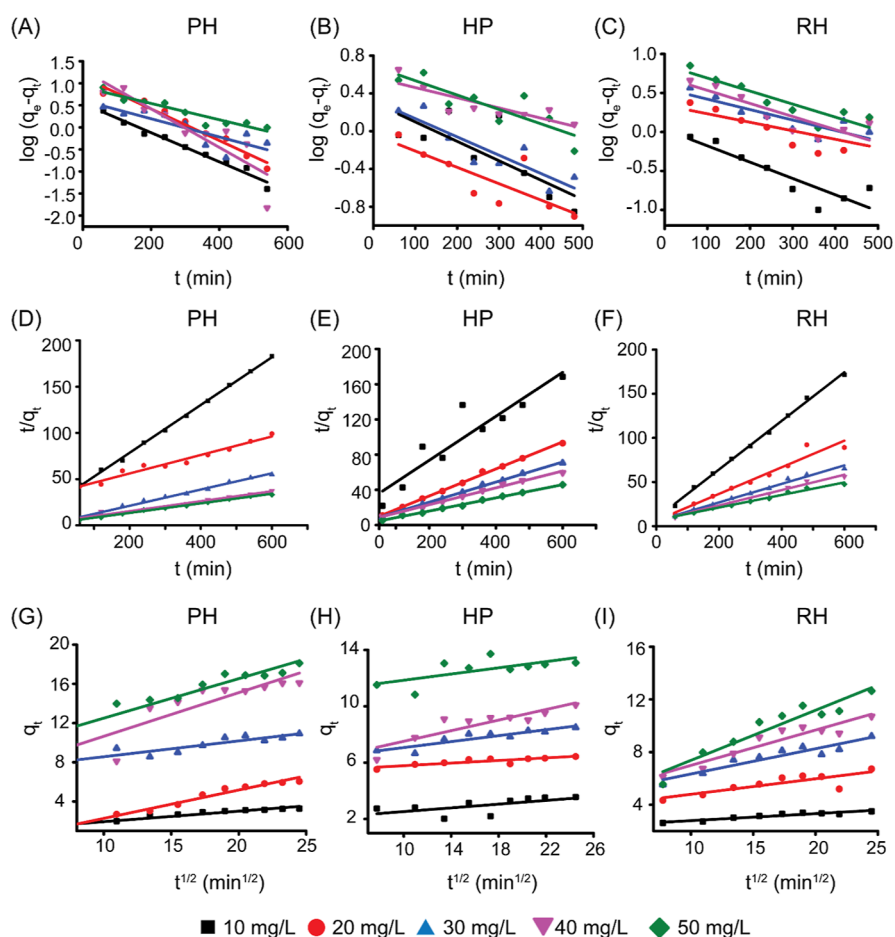
Figure 4. Adsorption kinetics during chromium adsorption. The graph (A−C) represents the pseudo-first order; the graph (D−F) represents the pseudo-second order; and the graph (G−I) represents the intra-particle diffusion plot for three hair samples (PH, HP, and RH, respectively). The adsorption data follows pseudo-second-order kinetics, suggesting the possibility of chemisorption.

Table 2. Estimated Values of Parameters for Different Kinetic Models

adsorbents	C_o (mg/L)	pseudo-first order			pseudo-second order			intraparticle diffusion		
		$K_1(min^{-1})$	$q_e(mg/g)$	R^2	$K_2(g/mg/min)$	$q_e(mg/g)$	R^2	$C(mg/g)$	$K_{id}(mg/g/min^{1/2})$	R^2
PH	10	0.457	1.719	0.974	0.04	3.87	0.997	0.868	0.107	0.89
	20	0.495	3.113	0.962	0.016	9.98	0.950	0.102	0.289	0.96
	30	0.270	1.754	0.615	0.046	11.38	0.985	6.954	0.161	0.78
	40	0.604	3.652	0.763	0.025	18.54	0.985	6.199	0.445	0.74
	50	0.255	2.489	0.885	0.029	19.31	0.985	8.469	0.403	0.87
HP	10	0.284	1.354	0.530	0.051	3.99	0.834	1.867	0.066	0.30
	20	0.275	0.963	0.596	0.102	6.50	0.997	5.317	0.046	0.72
	30	0.267	1.386	0.755	0.064	8.75	0.997	6.016	0.105	0.79
	40	0.149	1.76	0.665	0.048	10.44	0.982	5.635	0.188	0.76
	50	0.210	1.98	0.668	0.078	13.35	0.986	10.75	0.110	0.37
RH	10	0.004	1.032	0.760	0.091	3.628	0.997	2.256	0.053	0.88
	20	0.002	1.408	0.326	0.0059	6.63	0.950	3.161	0.117	0.65
	30	0.003	1.741	0.716	0.043	9.53	0.985	4.41	0.192	0.87
	40	0.038	2.018	0.173	0.035	11.50	0.985	4.302	0.268	0.87
	50	0.003	2.36	0.794	0.027	14.06	0.985	3.561	0.380	0.89

increased from 80 min (for 5 cm bed height) to 2460 min (20 cm bed height), resulting in more adsorption efficiency of the column and more Cr removal from the passing solution.[45] At the completion of the continuous column experiment, total Cr removed by the column was observed to be enhanced from 240 mg (at 5 cm bed height) to 1200 mg (at 20 cm bed height). It allows solution to get sufficient time to diffuse into

the adsorbents, thus staying in the column for longer time, thus treating a larger volume of effluents. In the initial phase of the experiment, adsorption sites of the adsorbent are freely available to bind with Cr, resulting in a negligible Cr concentration in eluting solution. Due to binding of Cr with the adsorbent, the bottom part of the column bed got saturated; thus, the adsorption zone gradually shifts toward the

Table 3. Percentage of Cr Removal after Regeneration

	percentage Cr removal after regeneration		
cycles	PH (% of Cr removal)	HP (% of Cr removal)	RH (% of Cr removal)
1	75.21	56.68	45.34
2	59.41	43.43	48.23
3	40.12	25.34	36.67
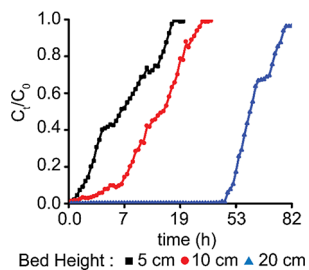
Figure 5. Effect of bed height on the breakthrough curve for Cr(VI) ion adsorption on human hair (C_0 = 50 mg/L, flow rate = 5 mL/min). C_0 and C_t represent the initial Cr(VI) concentration and Cr(VI) concentration at time t, respectively.

upper unsaturated part. As the column bed gets saturated, the Cr concentration in eluting solution increases gradually. The Cr concentration in eluting solution increases till the entire column bed (adsorption zone) gets saturated, and this time is referred to as the breakthrough time (T_b). Understandably, there is an increase in the breakthrough time when the bed height is increased.

Breakthrough time increased from 80 to 2640 min upon increase in bed height from 5 to 20 cm. Increase in bed height, therefore, results in relatively more Cr(VI) removal and increased column efficiency.

This study was conducted in two phases. In the first phase, we have investigated the Cr(VI) removal efficiency of five different adsorbent systems. In an earlier study, we reported a single-crystal organic nanoflower, 1,2-bis(tritylthio)ethane, with Cr(VI) adsorbance properties.[46] In phase 1 experiments, a hybrid material with 1,2-bis(tritylthio)ethane and magnetite showed enhanced Cr adsorbance compared to glass wool and 1,2-bis(tritylthio)ethane crystals. Interestingly, in phase 1 experiments, human hair showed maximum Cr(VI) removing ability, compared to other adsorbents. Mondal and Basu have earlier reported the utility of waste human hair toward removal of Cr(VI) from solution.[32] This prompted us to focus on various physical forms of human hair in a series of experiments, to further enhance its properties as cost-effective bio-adsorbents.

We have performed the experiments under different pH conditions ranging from 2 to 10. We observed that Cr(VI) adsorption at pH 2 is maximum in all the three hair forms tested. It may be because of the protonation of the adsorbent surfaces at low pH, which attracts more $HCrO_4^-$ and $Cr_2O_7^-$ ions. At higher pH, the electrostatic force of repulsion between OH^- and CrO_4^{2-} causes hindrance to the chromate ion to

bind to the adsorbent surface, resulting in lesser Cr adsorption.[46] Furthermore, the interaction between Cr(VI) and adsorbents was studied by using different isotherm and kinetic models. Among Langmuir, Freundlich, and D−R isotherm models, Cr(VI) adsorption by human hair fitted best with the Freundlich isotherm (R^2 = 0.99). The Freundlich isotherm model suggests the adsorption to be a reversible multi-layered process on heterogeneous surfaces. The value of n_F (adsorption intensity) represents the distribution of bonded metal ions on the surface of adsorbents, and $1/n_F$ in the range of 0 to 1 signifies the favorable condition for Cr(VI) adsorption on the adsorbent surface.[47] In the presented data, the value of $1/n_F$ lies in the range of 0 to 1, which support favorable adsorption conditions, and hence, multilayer adsorption is the dominating factor for Cr(VI) removal by human hair. The $1/n_F$ value less than 1 showed that significant Cr adsorption takes place at lower concentrations of adsorbents. A higher value of $1/n_F$ suggests a weak adsorption bond, leading to less metal adsorption.[48]

Kinetics of Cr(VI) interaction with human hair was studied by pseudo-first-order kinetics, pseudo-second-order kinetics, and intraparticle diffusion models. The data presented for Cr(VI) adsorption by human hair was best fitted with the pseudo-second-order kinetic model, which suggests chemisorption to be the rate-limiting step between the adsorbent and adsorbate.[49] Stronger interaction between the adsorbate and adsorbent is more in chemisorption compared to that in physical adsorption, leading to increase in adsorption capacity of the adsorbent.[50] The theoretical adsorption capacity obtained from pseudo-second-order kinetics [19.31 mg/g for PH, 14.01 mg/g for RH, and 10.44 mg/g for HP at a 50 mg/L Cr(VI) concentration] is close to the experimental adsorption capacity value (15.14 mg/g for PH, 13.27 mg/g for RH, and 10.5 mg/g for HP), suggesting chemisorption. Desorption and regeneration study of human hair suggests its potential for scaling up to commercial systems. Our results suggest that the Cr(VI) removing ability of all three forms decreased significantly from cycle 1 to cycle 3. The possible reason for the decrease in the removal capacity may be the modification in the morphology of adsorbents.[49] Continuous column experiment results showed increased Cr removal from 240 to 1200 mg when bed height increased from 5 to 20 cm. Increase in bed height results in more available active sites for Cr(VI) binding, which leads to enhanced column performance for Cr(VI) removal.

Table 4. Breakthrough Parameters at Different Bed Heights

bed height (cm)	C_0(mg/L)	M (g)	Q(mL/min)	T_b (min)	t_{total} (min)	q_{total} (mg)	$Q_{e(exp)}$(mg/g)	m_{total} (mg)	Y (%)	V_{eff} (mL)
5	50	4	5	80	960	190.70	47.67	240	96	4800
10	50	9	5	150	1800	447.3	49.7	450	97	9000
20	50	20	5	2640	4800	1156	57.80	1200	98	24000

CONCLUSIONS

This study focuses on the removal and reduction of Cr(VI) from wastewater. In this study, we have validated the Cr(VI) reduction efficiency of hybrid materials synthesized by magnetite and by 1,2-bis(tritylthio)ethane crystals. We observed that synthesized hybrid materials could reduce toxic Cr(VI) into non-toxic Cr(III) up to 90%. While screening the adsorption capacity of different adsorbents for Cr(VI) removal, we found that hybrid materials and 1,2-bis(tritylthio)ethane crystals have relatively low Cr(VI) removal efficiency, compared to human hair. This observation was the motivation to investigate the capacity of human hair and its various physical forms as a heavy metal adsorbent.

To explore the Cr removal efficiency of human hair, we have modified the human hair into three distinct physical forms; PH-by the ball milling process, HP-by pyrolysis, and RH-without any modification. The motive of employing different physical forms of human hair as a Cr adsorbent was to evaluate the Cr removal efficiency of physical and chemical modifications of hair. Moreover, human hair is an affordable bio-waste. Establishing human hair as a cost-effective Cr adsorbent could be a promising application, and it will reduce the toxic effects of chemicals formed as byproducts. We investigated the three forms of human hair PH, HP, and RH as a Cr adsorbent and performed a series of experiments to validate their adsorption capacity. Various parameters were investigated to understand the mechanism and kinetics of Cr(VI) removal. The adsorption capacity of PH was observed to be maximum (15.14 mg/g), followed by RH (13.27 mg/g) and HP (10.5 mg/g). The adsorption process was influenced by pH, and the maximum adsorption was observed at pH 2. Adsorption of Cr(VI) increases with an increase in the concentration of Cr(VI), and no significant increase in adsorption was observed after 3 h, indicating an optimum time of 3 h for typical Cr(VI) adsorption experimental cycles. An adsorption and desorption experiment were performed to validate the reusability of the adsorbent systems. The results suggest that for PH, efficiency of Cr(VI) removal decreased significantly from 75 to 40%, after three cycles. Kinetic studies were also performed to understand the adsorption process. Cr(VI) adsorption on human hair follows a pseudo-second-order kinetic model, suggesting chemisorption. From the adsorption study, it is clear that the use of a bio-waste like hair can be a simple, cost-effective, and efficient method for Cr removal and therefore can be scaled up to larger capacities.

EXPERIMENTAL SECTION

The chemicals and solvents used were of analytical-grade reagents. 1,2-Ethanedithiol was procured from Sigma-Aldrich. Ferrous sulphate heptahydrate, ferric nitrate, and diethyl ether were procured from Merck. Trityl chloride was procured from Sisco Research Laboratories Pvt. Ltd. Sodium dichromate dihydrate was procured from Fisher Scientific. Reagents for the pre-treatment of human hair (chloroform, diethyl ether, acetone, and methanol) were purchased from Merck. Hair samples were collected from the local market.

Synthesis of 1,2-Bis(tritylthio)ethane Crystals and Magnetite Nanoparticles. The synthesis of compound 1,2-bis(tritylthio)ethane crystals was done by incubating trityl chloride salts and EDT in the presence of TFA for 24 h. After 24 h, crystallization and further purification were performed by using diethyl ether. Magnetite nanoparticles were synthesized by co-precipitation of aqueous solutions of ferrous sulphate heptahydrate and ferric nitrate in the presence of citric acid followed by heating at 75 °C for 5 h. The synthesized magnetite nanoparticle was further washed with distilled water and desiccated at 60 °C.

Synthesis of Trityl-Magnetite Hybrid Materials. Synthesis of trityl-magnetite hybrid materials was performed by adapting an already published protocol.[36] Synthesized magnetite was dispersed in 0.2% diethyl ether. 0.5 mg/mL 1,2-bis(tritylthio)ethane was then added. Trityl-magnetite hybrid materials were formed after crystallization.

pH Stability of 1,2-Bis(tritylthio)ethane Crystals. To study the stability of 1,2-bis(tritylthio)ethane crystals at different pH, crystals were incubated in variable pH ranges ranging from 2 to 10, for 24 h. After 24 h, stability was checked by studying the changes in the morphology by using Jeol FESEM (model: JSM-7610F).

Pre-Treatment of Human Hair. The washed human hair samples were taken for the experiment as described elsewhere.[52] Human hair was cut into small fragments and washed thoroughly with distilled water four−five times. Washed samples were treated with an equal ratio of chloroform, methanol, acetone, and diethyl ether to remove extraneous substances. It was centrifuged at 10,000 rpm for 30 min, followed by supernatant removal and washing with distilled water. The washing process was repeated at least three times for complete removal of dirt and other extraneous materials, and the sample was desiccated at room temperature.

Modification of Human Hair. Washed and dried human hairs were pulverized employing an earlier reported protocol.[53] Washed and dried hairs were cut into small pieces (6−7 mm). Pulverization was performed in a ball mill apparatus (Fritsch Pulverisette 6). Size of the human hairs was reduced to 3−4 mm after pulverization. HP was obtained by the pyrolysis method which was performed in a muffle furnace at 200 °C. Three forms, PH, HP, and RH, were evaluated for their ability to adsorb Cr.

Characterization of Human Hair. Morphological characterization of the adsorbents was performed by FESEM (Jeol, JSM-7610F) before and after the adsorption experiments. The presence of Cr on the hair surface was also analyzed by EDX. FT-IR spectra of the adsorbent were recorded by using an FT-IR spectrophotometer in the 4000−400 cm⁻¹ range.

Adsorption Study. To estimate the Cr(VI) adsorption, various factors like the effect of different adsorbent doses, pH, the initial amount of Cr, and contact time were studied. To examine the effect of different adsorbent doses, 50 mg/L Cr(VI) solution was added in separate conical flasks containing different doses of human hair (0.5, 1, 2, 3, 4, 6, 8, and 10 g/L). Flasks were incubated at 25 °C for 10 h at 150 rpm. To analzse the effect of pH, 50 mg/L Cr(VI) solution under different pH conditions (from 2 to 10) was prepared and incubated at 25 °C for 10 h. To investigate the effect of different initial Cr concentrations and time, different flasks containing 100 mg of PH, HP, and RH with different Cr concentrations (10, 20, 30, 40, and 50 mg/L) were incubated at 25 °C and rotated at 150 rpm for 10 h. Cr solutions were collected at regular time intervals. The Cr concentration was estimated using an atomic emission spectrometer (MP AES 4210). The percentage and capacity of adsorption were determined by using the following equations

$$\% \text{ adsorption} = (C_0 - C_e)/C_0 \times 100$$

$$q_e = (C_o - C_e) \times V/M$$

where C_0 = initial concentration of the adsorbent, C_e = final concentration of the adsorbent, V = volume of the solution (in liters), and M = weight of the adsorbent (in grams).

Isotherm and Kinetic Studies. Different flasks containing 100 mg of the adsorbent and Cr(VI) solution of diverse concentrations 10, 20, 30, 40, and 50 mg/L were mixed gently and incubated at 25 °C and rotated at 150 rpm for 10 h. Cr adsorption at equilibrium was studied using Langmuir, Freundlich, and D−R isotherm models. The rate of adsorption was studied by pseudo-first-order and pseudo-second-order kinetics and intraparticle diffusion.

Desorption and Regeneration Study. Experiments for the study of desorption were conducted in the batch mode. The 50 mg/L concentration of Cr(VI)-saturated adsorbents was treated with 50 mL of water at pH 12, for 6 h.[54] Separated human hair was washed with distilled water. It was further regenerated on addition of 1 N HCl. Regenerated human hairs were washed with distilled water and desiccated at room temperature. The desorption percentage was calculated using the equation

$$\% \text{ desorption} = \frac{\text{concentration after elution}}{\text{concentration before elution}} \times 100$$

Column Study for Cr(VI) Adsorption. Continuous column experiments for Cr(VI) adsorption were performed with RH packed as a bed in a glass column of 2 cm internal diameter and 30 cm length. The RH-packed column was washed with deionized water and loaded with glass wool and then glass beads. A breakthrough curve was obtained with variable bed heights (5, 10, and 20 cm). Cr(VI) solution (50 mg/mL concentration) was passed through the RH-packed bed column using a peristaltic pump (PP-20-EX, Miclins, India) at a flow rate of 5 mL/min. The sample was collected at regular intervals, and the Cr(VI) concentration was estimated. Details of calculations with different column parameters are explained in the Supporting Information (Section 6).

ASSOCIATED CONTENT

Ⓢ Supporting Information

The Supporting Information is available free of charge at https://pubs.acs.org/doi/10.1021/acsomega.2c06268.

FESEM−EDX analysis of human hair, FT-IR analysis of human hair, relationship between q_e and C_e, relationship between q_t and t, and continuous column experimental setup (PDF)

AUTHOR INFORMATION

Corresponding Author

    Vibin Ramakrishnan − *Department of Biosciences and Bioengineering, Indian Institute of Technology Guwahati, Guwahati 781039 Assam, India;* ⓞ orcid.org/0000-0002-8048-3211; Email: vibin@iitg.ac.in

Authors

    Vivek Prakash − *Department of Biosciences and Bioengineering, Indian Institute of Technology Guwahati, Guwahati 781039 Assam, India*

    Kalpana Kumari − *Department of Biosciences and Bioengineering, Indian Institute of Technology Guwahati, Guwahati 781039 Assam, India*

Complete contact information is available at:
https://pubs.acs.org/10.1021/acsomega.2c06268

Author Contributions

V.P. performed the experiments. K.K. was involved in few analytical experiments, manuscript writing, and editing. V.R. supervised the project.

Notes

The authors declare no competing financial interest.

■ REFERENCES

(1) Bem, H.; Gallorini, M.; Rizzio, E.; Krzemińska, M. Comparative studies on the concentrations of some elements in the urban air particulate matter in Lodz City of Poland and in Milan, Italy. *Environ. Int.* **2003**, *29*, 423−428.

(2) Xu, C.; Qiu, B.; Gu, H.; Yang, X.; Wei, H.; Huang, X.; Wang, Y.; Rutman, D.; Cao, D.; Bhana, S.; Guo, Z.; Wei, S. Synergistic Interactions between Activated Carbon Fabrics and Toxic Hexavalent Chromium. *ECS J. Solid State Sci. Technol.* **2014**, *3*, M1.

(3) Qiu, B.; Gu, H.; Yan, X.; Guo, J.; Wang, Y.; Sun, D.; Wang, Q.; Khan, M.; Zhang, X.; Weeks, B. L.; Young, D. P.; Guo, Z.; Wei, S. Cellulose derived magnetic mesoporous carbon nanocomposites with enhanced hexavalent chromium removal. *J. Mater. Chem. A* **2014**, *2*, 17454−17462.

(4) Owlad, M.; Aroua, M. K.; Daud, W. A. W.; Baroutian, S. Removal of Hexavalent Chromium-Contaminated Water and Wastewater: A Review. *Water, Air, Soil Pollut.* **2009**, *200*, 59−77.

(5) Fu, F.; Wang, Q. Removal of heavy metal ions from wastewaters: a review. *J. Environ. Manage.* **2011**, *92*, 407−418.

(6) Liu, N.; Dai, W.; Fei, F.; Xu, H.; Lei, J.; Quan, G.; Zheng, Y.; Zhang, X.; Tang, L. J. S. Insights into the photocatalytic activation persulfate by visible light over ReS2/MIL-88B(Fe) for highly efficient degradation of ibuprofen: Combination of experimental and theoretical study. *Separ. Purif. Technol.* **2022**, *297*, 121545.

(7) Liu, N.; Fei, F.; Dai, W.; Lei, J.; Bi, F.; Wang, B.; Quan, G.; Zhang, X.; Tang, L. Visible-light-assisted persulfate activation by SnS2/MIL-88B (Fe) Z-scheme heterojunction for enhanced degradation of ibuprofen. *J. Colloid Interface Sci.* **2022**, *625*, 965−977.

(8) Esmaeili, A.; Hejazi, E.; Vasseghian, Y. Comparison study of biosorption and coagulation/air flotation methods for chromium removal from wastewater: experiments and neural network modeling. *RSC Adv.* **2015**, *5*, 91776−91784.

(9) Bharath, G.; Hai, A.; Rambabu, K.; Savariraj, D.; Ibrahim, Y.; Banat, F. The fabrication of activated carbon and metal-carbide 2D framework-based asymmetric electrodes for the capacitive deionization of Cr(vi) ions toward industrial wastewater remediation. *Environ. Sci.: Water Res. Technol.* **2020**, *6*, 351−361.

(10) Zhu, Z.; Rao, R.; Zhao, Z.; Chen, J.; Jiang, W.; Bi, F.; Yang, Y.; Zhang, X. Research progress on removal of phthalates pollutants from environment. *J. Mol. Liq.* **2022**, *355*, 118930.

(11) Ren, G.; Han, H.; Wang, Y.; Liu, S.; Zhao, J.; Meng, X.; Li, Z. Recent Advances of Photocatalytic Application in Water Treatment: A Review. *Nanomaterials* **2021**, *11*, 1804.

(12) Cui, H.; Huang, X.; Yu, Z.; Chen, P.; Cao, X. Application progress of enhanced coagulation in water treatment. *RSC Adv.* **2020**, *10*, 20231−20244.

(13) Abdel-Tawwab, M.; El-Sayed, G. O.; Shady, S. H. H. Capability of some agricultural wastes for removing some heavy metals from

polluted water stocked in combination with Nile tilapia, Oreochromis niloticus (L.). *Int. Aquat. Res.* **2017**, *9*, 153−160.

(14) Maddaloni, M.; Alessandri, I.; Vassalini, I. Food-waste enables carboxylated gold nanoparticles to completely abat hexavalent chromium in drinking water. *Environ. Nanotechnol., Monit. Manage.* **2022**, *18*, 100686.

(15) Wang, Y.; Gong, Y.; Lin, N.; Yu, L.; Du, B.; Zhang, X. Enhanced removal of Cr (VI) from aqueous solution by stabilized nanoscale zero valent iron and copper bimetal intercalated montmorillonite. *J. Colloid Interface Sci.* **2022**, *606*, 941−952.

(16) Zheng, X.; Zhao, B.; Liu, C. Bio-reduction mechanism of V(V) by thermophilic hydrogen-producing bacteria under acidic conditions. *Environ. Sci.: Water Res. Technol.* **2021**, *7*, 1657−1665.

(17) Tan, J.; Song, Y.; Huang, X.; Zhou, L. Facile functionalization of natural peach gum polysaccharide with multiple amine groups for highly efficient removal of toxic hexavalent chromium (Cr (VI)) ions from water. *ACS Omega* **2018**, *3*, 17309−17318.

(18) Zhou, L.; Duan, Y.; Xu, X. Facile preparation of amine-rich polyamidoamine (PAMAM) gel for highly efficient removal of Cr (VI) ions. *Colloids Surf., A* **2019**, *579*, 123685.

(19) Wang, Y.; Gong, Y.; Lin, N.; Jiang, H.; Wei, X.; Liu, N.; Zhang, X. Cellulose hydrogel coated nanometer zero-valent iron intercalated montmorillonite (CH-MMT-nFe0) for enhanced reductive removal of Cr (VI): Characterization, performance, and mechanisms. *J. Mol. Liq.* **2022**, *347*, 118355.

(20) Wang, Y.; Yu, L.; Wang, R.; Wang, Y.; Zhang, X. A novel cellulose hydrogel coating with nanoscale Fe0 for Cr (VI) adsorption and reduction. *Sci. Total Environ.* **2020**, *726*, 138625.

(21) Sasidharan, S.; Ramakrishnan, V. Aromatic interactions directing peptide nano-assembly. *Adv. Protein Chem. Struct. Biol.* **2022**, *130*, 119−160.

(22) Pandey, G.; Ramakrishnan, V. Invasive and non-invasive therapies for Alzheimer's disease and other amyloidosis. *Biophys. Rev.* **2020**, *12*, 1175−1186.

(23) Sasidharan, S.; Hazam, P. K.; Ramakrishnan, V. Symmetry-Directed Self-Organization in Peptide Nanoassemblies through Aromatic π−π Interactions. *J. Phys. Chem. B* **2017**, *121*, 404−411.

(24) Prakash, V.; Christian, Y.; Redkar, A. S.; Roy, A.; Anandalakshmi, R.; Ramakrishnan, V. Antibacterial hydrogels of aromatic tripeptides. *Soft Matter* **2022**, *18*, 6360−6371.

(25) Saikia, J.; Dharmalingam, K.; Anandalakshmi, R.; Redkar, A. S.; Bhat, V. T.; Ramakrishnan, V. Electric field modulated peptide based hydrogel nanocatalysts. *Soft Matter* **2021**, *17*, 9725−9735.

(26) Pandey, G.; Saikia, J.; Sasidharan, S.; Joshi, D. C.; Thota, S.; Nemade, H. B.; Chaudhary, N.; Ramakrishnan, V. Modulation of Peptide Based Nano-Assemblies with Electric and Magnetic Fields. *Sci. Rep.* **2017**, *7*, 2726.

(27) Prakash, V.; Mukesh, B.; Sasidharan, S.; Redkar, A. S.; Roy, A.; Anandalakshmi, R.; Ramakrishnan, V. Syndiotactic hexamer peptide nanodots. *Eur. Biophys. J.* **2022**, *51*, 483−491.

(28) Saikia, J.; Bhat, V. T.; Potnuru, L. R.; Redkar, A. S.; Agarwal, V.; Ramakrishnan, V. Minimalist De Novo Design of an Artificial Enzyme. *ACS Omega* **2022**, *7*, 19131−19140.

(29) Sasidharan, S.; Ghosh, S.; Sreedhar, R.; Kumari, K.; Thota, S.; Ramakrishnan, V. Anisotropic Ferromagnetic Organic Nanoflowers. *J. Phys. Chem. C* **2022**, *126*, 8511−8518.

(30) Sasidharan, S. P. S.; Chaudhary, N.; Ramakrishnan, V. Single Crystal Organic Nanoflowers. *Sci. Rep.* **2017**, *7*, 17335.

(31) Ingole, D. N.; Burghate, S. Adsorption of Oil from Waste Water by Using Human Hair. *J. Environ. Sci. Comput. Sci. Eng. Technol.* **2014**, *3*, 207−2017.

(32) Mondal, N. K.; Basu, S. Potentiality of waste human hair towards removal of chromium(VI) from solution: kinetic and equilibrium studies. *Appl. Water Sci.* **2019**, *9*, 49.

(33) Gomberg, M. An instance of trivalent carbon: Triphenylmethyl. *J. Am. Chem. Soc.* **1900**, *22*, 757−771.

(34) He, Y. T.; Traina, S. J. Cr(VI) Reduction and Immobilization by Magnetite under Alkaline pH Conditions: The Role of Passivation. *Environ. Sci. Technol.* **2005**, *39*, 4499−4504.

(35) Pan, Z.; Zhu, X.; Satpathy, A.; Li, W.; Fortner, J. D.; Giammar, D. E. Cr(VI) Adsorption on Engineered Iron Oxide Nanoparticles: Exploring Complexation Processes and Water Chemistry. *Environ. Sci. Technol.* **2019**, *53*, 11913−11921.

(36) Peterson, M. L.; Brown, G. E.; Parks, G. A. Direct XAFS evidence for heterogeneous redox reaction at the aqueous chromium/ magnetite interface. *Colloids Surf., A* **1996**, *107*, 77−88.

(37) Meena, A. H.; Arai, Y. Effects of common groundwater ions on chromate removal by magnetite: importance of chromate adsorption. *Geochem. Trans.* **2016**, *17*, 1.

(38) Patra, C.; Shahnaz, T.; Subbiah, S.; Narayanasamy, S. Comparative assessment of raw and acid-activated preparations of novel Pongamia pinnata shells for adsorption of hexavalent chromium from simulated wastewater. *Environ. Sci. Pollut. Res. Int.* **2020**, *27*, 14836−14851.

(39) Pienpinijtham, P.; Thammacharoen, C.; Naranitad, S.; Ekgasit, S. Analysis of cosmetic residues on a single human hair by ATR FT-IR microspectroscopy. *Spectrochim. Acta, Part A* **2018**, *197*, 230−236.

(40) Hamadi, N. K.; Chen, X. D.; Farid, M. M.; Lu, M. G. Q. Adsorption kinetics for the removal of chromium(VI) from aqueous solution by adsorbents derived from used tyres and sawdust. *Chem. Eng. J.* **2001**, *84*, 95−105.

(41) Mohamed, A.; Nasser, W. S.; Osman, T. A.; Toprak, M. S.; Muhammed, M.; Uheida, A. Removal of chromium (VI) from aqueous solutions using surface modified composite nanofibers. *J. Colloid Interface Sci.* **2017**, *505*, 682−691.

(42) Albadarin, A. B.; Mangwandi, C.; Al-Muhtaseb, A. a. H.; Walker, G. M.; Allen, S. J.; Ahmad, M. N. M. Kinetic and thermodynamics of chromium ions adsorption onto low-cost dolomite adsorbent. *Chem. Eng. J.* **2012**, *179*, 193−202.

(43) Nagaraj, A.; Munusamy, M. A.; Al-Arfaj, A. A.; Rajan, M. Functional Ionic Liquid-Capped Graphene Quantum Dots for Chromium Removal from Chromium Contaminated Water. *J. Chem. Eng. Data* **2019**, *64*, 651−667.

(44) Ghasemi, M.; Naushad, M.; Ghasemi, N.; Khosravi-fard, Y. Adsorption of Pb(II) from aqueous solution using new adsorbents prepared from agricultural waste: Adsorption isotherm and kinetic studies. *J. Ind. Eng. Chem.* **2014**, *20*, 2193−2199.

(45) Sadaf, S.; Bhatti, H. N. Evaluation of peanut husk as a novel, low cost biosorbent for the removal of Indosol Orange RSN dye from aqueous solutions: batch and fixed bed studies. *Clean Technol. Environ. Policy* **2014**, *16*, 527−544.

(46) Anah, L.; Astrini, N. Influence of pH on Cr(VI) ions removal from aqueous solutions using carboxymethyl cellulose-based hydrogel as adsorbent. *IOP Conf. Ser. Earth Environ. Sci.* **2017**, *60*, 012010.

(47) E, S.; N, S.; Patra, C.; Varghese, L. A.; N, S. Biosorption potential of Gliricidia sepium leaf powder to sequester hexavalent chromium from synthetic aqueous solution. *J. Environ. Chem. Eng.* **2019**, *7*, 103112.

(48) Aziz, H. A.; Yusoff, M. S.; Adlan, M. N.; Adnan, N. H.; Alias, S. Physico-chemical removal of iron from semi-aerobic landfill leachate by limestone filter. *Waste Manag.* **2004**, *24*, 353−358.

(49) Kumar, S.; Shahnaz, T.; Selvaraju, N.; Rajaraman, P. V. Kinetic and thermodynamic studies on biosorption of Cr(VI) on raw and chemically modified Datura stramonium fruit. *Environ. Monit. Assess.* **2020**, *192*, 248.

(50) Vo, T. S.; Hossain, M. M.; Jeong, H. M.; Kim, K. Heavy metal removal applications using adsorptive membranes. *Nano Convergence* **2020**, *7*, 36.

(51) Zhang, J.; Shang, T.; Jin, X.; Gao, J.; Zhao, Q. Study of chromium(vi) removal from aqueous solution using nitrogen-enriched activated carbon based bamboo processing residues. *RSC Adv.* **2015**, *5*, 784−790.

(52) Nakamura, A.; Arimoto, M.; Takeuchi, K.; Fujii, T. A rapid extraction procedure of human hair proteins and identification of phosphorylated species. *Biol. Pharm. Bull.* **2002**, *25*, 569.

(53) da Rosa Chagas, A. G.; Spinelli, E.; Fiaux, S. B.; da Silva Barreto, A.; Rodrigues, S. V. Particle-size distribution (PSD) of pulverized hair: A quantitative approach of milling efficiency and its

correlation with drug extraction efficiency. *Forensic Sci. Int.* **2017**, *277*, 188−196.

(54) Nagaraj, A.; Munusamy, M. A.; Al-Arfaj, A. A.; Rajan, M. Functional Ionic Liquid-Capped Graphene Quantum Dots for Chromium Removal from Chromium Contaminated Water. *J. Chem. Eng. Data* **2019**, *64*, 651−667.